Computations and Materials in Civil Engineering
2017, Volume 2, No. 1, 1-15

Golden Spiral Publishing Inc.
http://gspiralpublishing.com/index.php/cmce

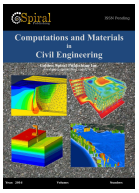

Research Paper

# The axisymetric failure mechanism of circular shallow foundations and pile foundations in non-cohesive soils

Stefan Van Baars[a,1]
[a] *Faculty of Science and Technology, University of Luxembourg, Luxembourg, Luxembourg*
(Received 27 March 2017; accepted 9 September 2017)

**Abstract.** In 1920 Prandtl published an analytical solution for the bearing capacity of a centric loaded strip footing on a weightless in-finite half-space, based on a so-called Prandtl-wedge failure mechanism. Reissner extended this solution for a surrounding surcharge and Keverling Buisman and Terzaghi for the soil weight. Meyerhof and other researchers presented correction factors for the shape of the shallow foundation, which would suggest that, the failure mechanism of circular shallow foundations, is related to the Prandtl-wedge failure mechanism. Meyerhof and Koppejan adapted this Prandtl-wedge failure mechanism also for pile foundations. The numerical calculations made in this article show that the Prandtl-wedge cannot be applied to circular shallow foundations and pile foundations in non-cohesive soils. The failure zone (plastic zone) below a loaded circular plate or pile tip, is far wider and deeper than the Prandtl-wedge. The calculations also show that there is, for these axisymmetric cases, failure both in and out of the standard *x-y* plane, but most of the failure is due to out-of-plane (tangential) failure. Therefore, this failure mechanism is different from the Prandtl-wedge failure mechanism. Also interesting are the circular and diagonal thin zones below the plate and around the pile tip, where there is no out-of-plane failure, although there is still in-plane failure. In these thin zones without out-of-plane failure, the tangential (out-of-plane) stresses are relatively high due to large shear strains, formed during previous shearing or sliding of the soil.

**Keywords:** Bearing capacity; Footings; Foundations; Finite Element Modelling.

## 1. Introduction

In 1920, Ludwig Prandtl published an analytical solution for the bearing capacity of a soil under a load, $p$, causing kinematic failure of the weightless infinite half-space underneath. The strength of the half-space is given by the angle of internal friction, $\phi$, and the cohesion, $c$. The failure mechanism proposed by Prandtl (see the original drawing of Prandtl in Figure 1) has been validated by laboratory tests, for example those performed by Jumikis (1956), Selig and McKee (1961), and Muhs and Weiß (1972).

Prandtl subdivided the sliding soil part into three zones:

1. Zone 1: A triangular zone below the strip load. Since there is no friction on the ground surface, the directions of the principal stresses are horizontal and vertical; the largest principal stress is in the vertical direction.

[1]Corresponding author.
stefan.vanbaars@uni.lu

2. Zone 2: A wedge with the shape of a logarithmic spiral, in which the principal stresses rotate through $90°$, from Zone 1 to Zone 3. The pitch of the sliding surface equals the angle of internal friction; $\xi = \phi$, creating a smooth transition between Zone 1 and Zone 3.
3. Zone 3: A triangular zone adjacent to the strip load. Since there is no friction on the surface of the ground, the directions of principal stress are horizontal and vertical; the largest principal stress is in the horizontal direction.

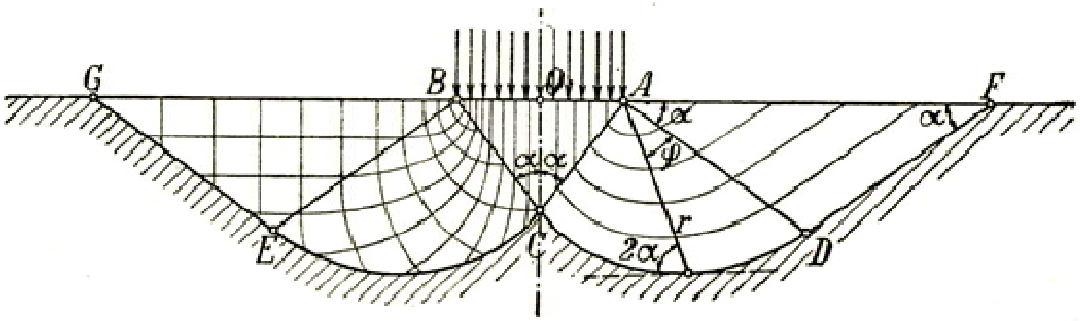


Fig. 1. The Prandtl-wedge failure mechanism (Prandtl, 1920).

The solution of Prandtl was extended by Hans J. Reissner (1924) for a surrounding surcharge, $q$, and was based on the same failure mechanism. Albert S. Keverling Buisman (1940) and Karl Terzaghi (1943) extended the Prandtl-Reissner formula for the soil weight, $\gamma$. It was Terzaghi (1943) who wrote the equation for the bearing capacity as a superposition of the three separate bearing capacity components:

$$p_v = cN_c + qN_q + \tfrac{1}{2}\gamma BN_\gamma \tag{1}$$

where $N_c$, $N_q$, $N_\gamma$ are the bearing capacity coefficients for respectively the cohesion, surcharge and soil-weight (-), $c$ is the cohesion (kPa), $q$ is the surcharge (kPa), $\gamma$ is the effective soil weight (kN/m$^3$) and $B$ is the width of the strip load (m).

The cohesion bearing capacity factor follows from the solution of Prandtl (1920):

$$N_c = \left(K_p \cdot e^{\pi \tan\phi} - 1\right)\cot\phi \quad \text{with:} \quad K_p = \frac{1+\sin\phi}{1-\sin\phi} \tag{2}$$

where $\phi$ is the friction angle of the soil and $K_p$ is the passive earth pressure coefficient (-).

The surcharge bearing capacity factor follows from the solution of Reissner (1924):

$$N_q = K_p \cdot \left(\frac{r_3}{r_1}\right)^2 = K_p \cdot e^{\pi \tan\phi} \quad \text{with:} \quad K_p = \frac{1+\sin\phi}{1-\sin\phi} \tag{3}$$

Keverling Buisman (1940), Terzaghi (1943), Caquot and Kérisel (1953), Meyerhof (1951; 1953; 1963; 1965), Brinch Hansen (1970), Vesic (1973, 1975), and Chen (1975) subsequently proposed different equations for the soil-weight bearing capacity factor $N_\gamma$. Therefore the following equations for the soil-weight bearing capacity factor can be found in the literature:

$$
\begin{aligned}
N_\gamma &= \left(K_p \cdot e^{\pi \tan\phi} - 1\right)\tan\left(1.4\phi\right) \quad \text{(Meyerhof, 1963)},\\
N_\gamma &= 1.5\left(K_p \cdot e^{\pi \tan\phi} - 1\right)\tan\phi \quad \text{(Brinch Hansen, 1970)},\\
N_\gamma &= 2\left(K_p \cdot e^{\pi \tan\phi} + 1\right)\tan\phi \quad \text{(Vesic, 1973)},\\
N_\gamma &= 2\left(K_p \cdot e^{\pi \tan\phi} - 1\right)\tan\phi \quad \text{(Chen, 1975)}.
\end{aligned} \tag{4}
$$

There is however, a clear difference in bearing capacity between the numerical and analytical solutions, especially for higher friction angles. The reason for this is that the solutions of Equations 2, 3 and 4 are all based on extreme dilatant (associated) soil, for which the dilatancy angle $\psi = \phi$. Loukidis et al. (2008) already noticed, from their numerical calculations, that non-dilatant (i.e. non-associated) soil is 15% - 30% weaker (lower bearing capacity factors) than extreme dilatant soil, and it has also a rougher (less steady) failure pattern. This difference between the (extreme dilatant or associated) analytical solutions and the (non-dilatant or non-associated) numerical results, has been explained by Knudsen and Mortensen (2016): The higher the friction angle, the wider the logarithmic spiral (larger pitch) of the Prandtl-wedge and the more the stresses reduce during failure. Therefore, the analytical formulas are only kinematically admissible for associated flow. The problem of associated soil is that its high dilatancy angle is very unrealistic for natural soils. Especially for higher friction angles, the error in the calculated bearing capacity factor, is very high for non-dilatant soils, so it is better to use numerically derived bearing capacity factors, for example, as presented by Van Baars (2015, 2016):

$$
\begin{aligned}
N_q &= \cos^2\phi \cdot K_p \cdot \mathrm{e}^{\pi \tan\phi}\\
N_c &= \left(N_q - 1\right)\cot\phi\\
N_\gamma &= 2\left(K_p \cdot e^{\pi \tan\phi} + 1\right)\tan\phi \quad \text{(Rough plate: Vesic)}\\
N_\gamma &= 4\tan\phi \cdot \left(e^{\pi \tan\phi} - 1\right) \qquad \text{(Smooth plate)}
\end{aligned} \tag{5}
$$

George G. Meyerhof (1953) was the first to propose equations for inclined loads. He was also the first in 1963 to write the formula for the (vertical) bearing capacity $p_v$ with dimensionless bearing capacity factors ($N$), inclination factors ($i$) and shape factors ($s$), for the three independent bearing components: cohesion ($c$), surcharge ($q$) and soil-weight ($\gamma$):

$$p_v = i_c s_c c N_c + i_q s_q q N_q + i_\gamma s_\gamma \tfrac{1}{2}\gamma B N_\gamma. \tag{6}$$

Jørgen A. Brinch Hansen (1970) also adopted this formula, which is still used nowadays. If the shape of the foundation area is not an infinitely long strip, but a rectangular area, of width $B$ and length $L$ (where it is assumed, that the width is the shortest dimension, i,e, $L \geq B$), correction factors for the shape are used. Meyerhof (1963) was the first to publish shape factors:

$$s_q = s_\gamma = 1 + 0.1K_p\frac{B}{L}\sin\phi, \quad s_c = 1 + 0.2K_p\frac{B}{L} \quad \text{with:} \quad K_p = \frac{1+\sin\phi}{1-\sin\phi} \tag{7}$$

A few years later, De Beer (1967, 1970) published his shape factors, based on laboratory experiments. Brinch Hansen (1970) based his shape factors on the experimental results of De Beer. So the most commonly used shape factors are (for $B \leq L$):

$$s_c = 1 + 0.2\frac{B}{L}, \quad s_q = 1 + \frac{B}{L}\sin\phi, \quad s_\gamma = 1 - 0.3\frac{B}{L}. \tag{8}$$

In practice for circular shallow foundations, it is assumed that there is no difference with square foundations ($B/L = 1$). Knudsen and Mortensen (2016) compared for friction-less soils ($\phi = 0$), the bearing capacity for axisymmetric (2D Plaxis), circular, and square foundations (both 3D Plaxis). They found very similar results (deviation less than 3%). This means that the shape factors can also be studied with axisymmetric calculations.

From several publications, for example Zhu and Michalowski (2005), and Tapper et al. (2015), it follows that the shape factors are related to $\sqrt{\frac{B}{L}}$, and not to $\frac{B}{L}$. Van Baars (2015) proposed therefore the following shape factors, based on axisymmetric finite element calculations on non-dilatant soils:

$$\begin{aligned} s_c &= 1 - \left(0.7 - 0.5\tan\phi\right)\cdot\sqrt{\frac{B}{L}}, \\ s_q &= 1 - \left(0.7 - \frac{2}{3}\tan\phi\right)\cdot\sqrt{\frac{B}{L}}, \\ s_\gamma &= 1 - \left(0.6 - \exp(-\frac{\phi}{4^\circ}\right)\cdot\sqrt{\frac{B}{L}}. \end{aligned} \tag{9}$$

## 2. Axisymmetric failure versus plane strain failure

The use of shape factors would suggest that only a certain small correction is needed to go from the Prandtl-wedge plane strain failure mechanism to an axisymmetric failure mechanism. Since this is unclear, the main purpose of this study is to check the failure mechanism for axial-symmetric foundations.

There is a risk in assuming a Prandtl-wedge shaped failure mechanism for circular shaped loaded areas, such as for example Figure 2. The resulting shape factors would be far too high, according to Finite Element calculations of Van Baars (2014, 2015, 2016), but also according to the laboratory tests of De Beer. The reason for this is that the ground surface area of zone 3 of the Prandtl wedge (i.e. the triangular shaped zone not below but adjacent to the load), becomes too big, creating too much support, so before this Prandtl-wedge failure mechanism can occur, already another mechanism occurs.

For the strip load (plane strain failure) the lowest principal stress, in zone 3 of the wedge, is the vertical stress, which is zero without a surcharge, and the largest principal stress is the horizontal stress (perpendicular to the load).

For the circular load (axisymmetric failure) however, the lowest principal stress, in zone 3 of the wedge, is not the vertical stress, but the tangential stress (out of the *x-y* plane), which can be even zero. Due to this cleaving failure mechanism, the bearing capacity of a circular load will be far less than of a strip load, resulting in shape factors below "1". Therefore an adittional purpose of this study is to check the out-of-plane stresses for axi-symmetric foundations.

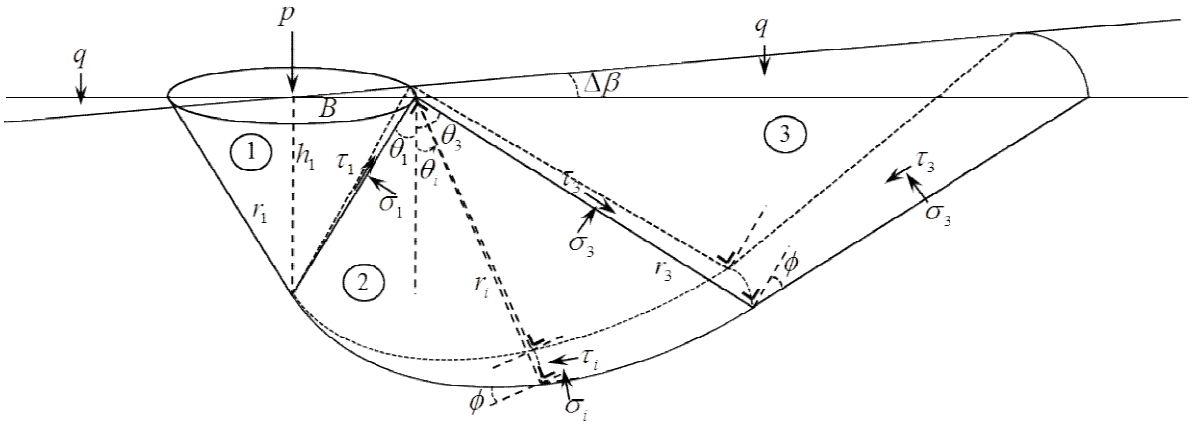


Fig. 2 Prandtl-wedge approach for circular loaded areas.

The success of the analytical solution for shallow foundations inspired researchers to try something similar for pile foundations. The first who applied the Prandtl-wedge for pile foundations were Keverling Buisman (1935, 1940) and Meyerhof (1951), but they forgot about the shape factors, because these were first published by Meyerhof in 1963. Meyerhof proposed a failure mechanism near the pile tip, which is a sort of Prandtl-wedge type failure, but with, instead of a triangular shaped zone 3, an extended logarithmic spiral shaped zone 2, which continues all the way up to the pile shaft, see the right side of Figure 3.

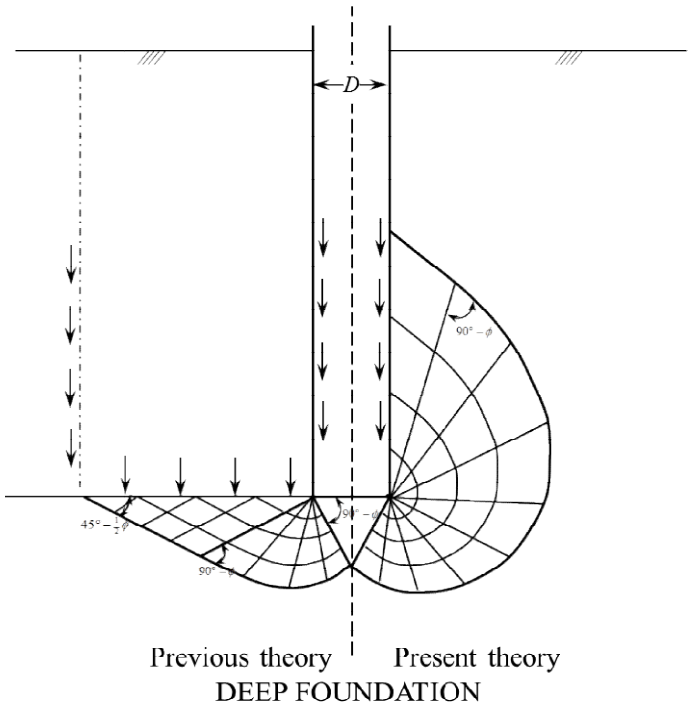


Fig. 3. Prandtl-wedge failure near a pile tip (Meyerhof, 1951).

Other researchers, for example Van Mierlo & Koppejan (1952) and Caquot and Kerisel (1966) have adopted this extended logarithmic spiral shape failure mechanism around the

pile tip. For the determination of the bearing capacity of the tip of a foundation pile nowadays, still the general this concept of Meyerhof is used, see for example Vesic, 1967, or Fang, 1990.

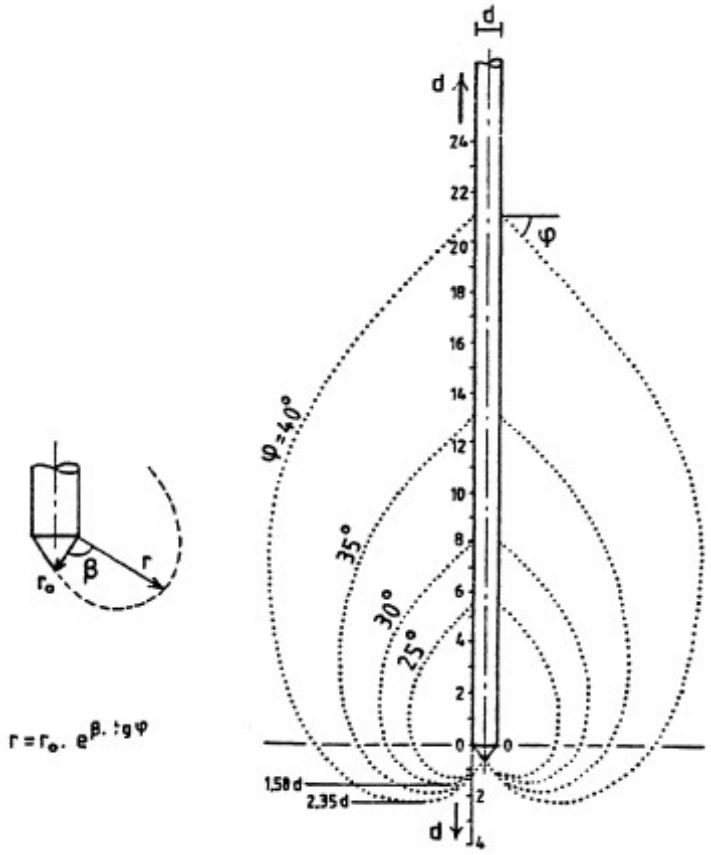


Fig. 4. Logarithmic spiral shape failure mechanism around a pile tip (Van Mierlo & Koppejan, 1952).

In many countries, the design of the pile bearing capacity is based on the bearing capacity ($q_c$-value) measured with the cone of the Cone Penetration Test (CPT). The thin CPT cone, as a model test, has a smaller diameter $D$ and is unfortunately far more sensitive for the discontinuities of the subsoil as real piles. Therefore, every CPT-based method needs a rule for "smoothening" the measured discontinuities over a certain distance. The distance over which this "smoothening" rule must be applied is, in case of the Koppejan's method (Van Mierlo & Koppejan, 1952), based on this logarithmic spiral shape failure mechanism, see Figure 4. Because of this logarithmic spiral, the failure zone is, in the Koppejan's method, assumed to reach from 0,7 $D$ to 4 $D$ below the pile tip, until 8 $D$ above the pile tip.

This failure mechanism is however incorrect. Although the soil, below the level of the pile tip, can rotate away from the pile, a slip failure along this logarithmic spiral, above the level of the pile tip, is impossible, since this soil cannot rotate towards the pile and will not finally disappear in the pile.

Laboratory model tests, see Figure 5, and numerical simulations show another failure mechanism: a global, balloon shaped, failure zone. The failure zone is mostly below, and

not above, the level of the pile tip; from 5 to 6 $D$ below the pile tip, until 2 or 3 $D$ above the pile tip for a fully elasto-plastic soil (for example in Figure 9). This shows that it is not correct to assume a Prandtl-wedge type failure mechanism near the tip of a foundation pile, or to derive the smoothing zone from the shape of a logarithmic spiral.

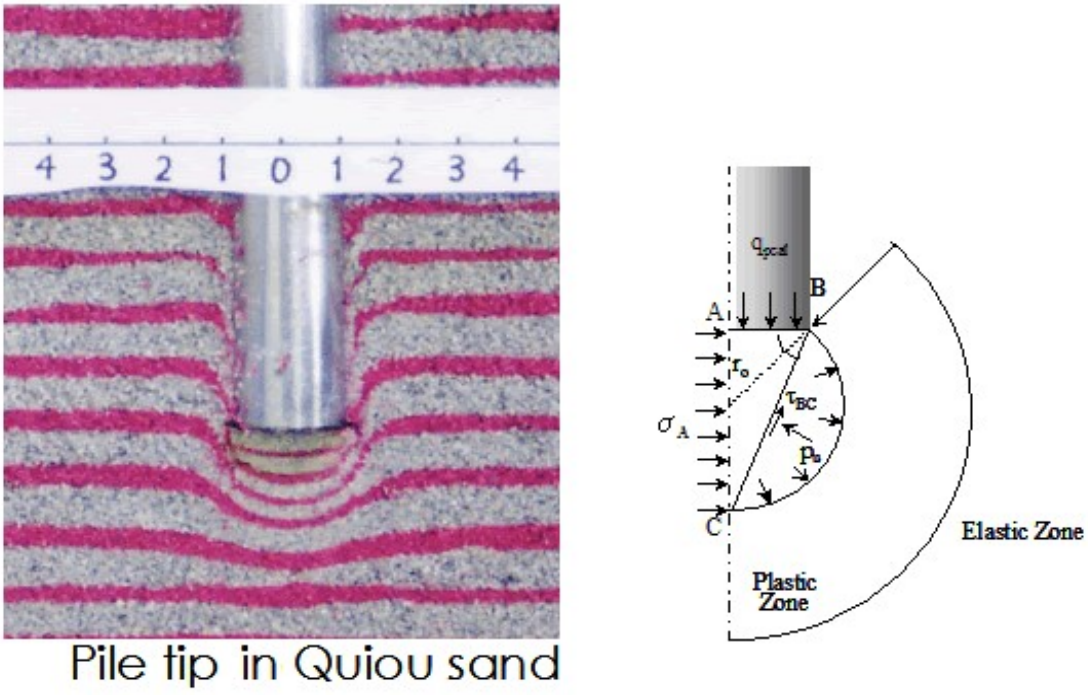


Fig. 5. Global failure below pile tip in crushable sand.

(Picture from Kyushu University, Geotechnical Engineering Research Group)

## 3. Failure mechanism of circular shallow foundations

### 3.1. *Numerical simulation*

In order to check the axisymmetric failure mechanism for shallow foundations, finite element model calculations have been made with Plaxis 2D. A Mohr-Coulomb soil model has been used for a fine, wide mesh with 15-node elements. The soil has a Young's modulus of $E$ = 50 MPa and a Poisson's ratio of $\nu$ = 0.3. The groundwater level is at the surface.

The used plate for the shallow foundation has been simulated with a displacement-controlled calculation, in which the horizontal displacements are fixed below the plate, creating an infinite stiff and rough plate. The plate has a radius of 2.0 m.

### 3.2. *Results: in-plane versus out-of-plane failure zones*

For shallow foundations, there are three different bearing capacity components: the cohesion, the surcharge and the soil-weight. Since the focus is on non-cohesive materials, the cohesion component will not be discussed here.

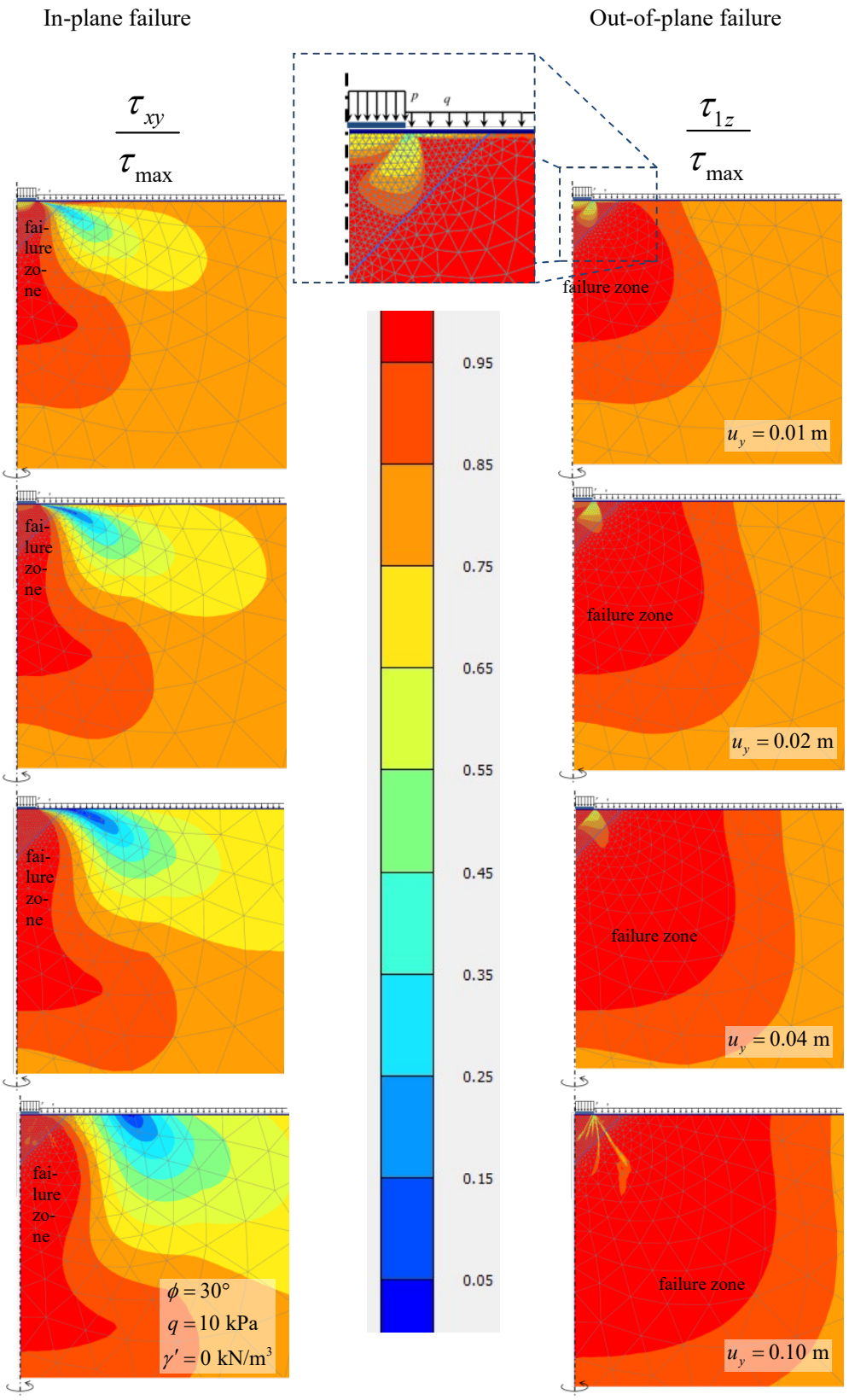


Fig. 6. Surcharge Case: Relative shear stress (left: in-plane; right: out-of-plane).

The surcharge component is studied by using a non-cohesive soil with a zero effective weight. Figure 6 shows, for a circular shallow foundation, with adjacent surcharge *q*, the relative shear stresses for both the *x-y* plane, and also out of this plane, so for a plane including the tangential *z*-direction, or "out-of-plane" direction. This figure shows that the failure zone (plastic zone) is far wider and deeper than the Prandtl-wedge. It also shows that there is failure both in and out of the standard *x-y* plane, but most of the failure is due to out-of-plane failure (this failure zone is much bigger). Therefore, the axisymmetric failure mechanism is different from the Prandtl-wedge failure mechanism. Since Plaxis 2D does not distinguish for its plots between out-of-plane and in-plane failure, a User Defined Soil Model has been programmed as a Dynamic Link Library in which the, out-of-plane and in-plane, relative normal and shear stress ratios were defined as State Parameters, which can be plotted in Plaxis.

### 3.3. *Results: relative tangential stress versus relative shear stress*

Figure 7 shows on the right again a detailed plot of the relative out-of-plane shear stress, which indicates that most of the soil is failing. Near the loaded circular foundation plate, there are only some thin zones not failing. Figure 7 shows on the left the relative tangential (out-of-plane) stress $\sigma_{zz}$. This stress is in most cases as low as the lowest principal stress $\sigma_3$, but near the loaded circular foundation plate, there are some thin zones where the tangential stress $\sigma_{zz}$ is even as high as the highest principal stress $\sigma_1$.

Figure 7 shows that the thin zones which are not failing, are exactly the zones where the tangential stress $\sigma_{zz}$ is as high as the highest principal stress $\sigma_1$. These zones were formed during former internal (in plane) sliding during loading.

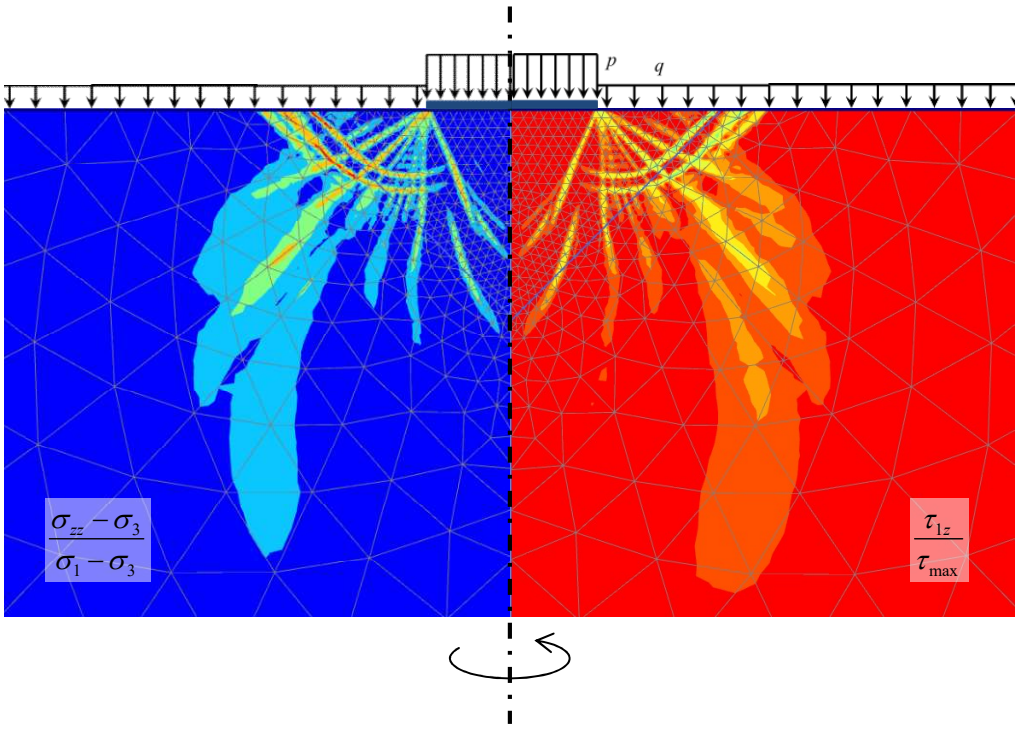


Fig. 7. Out-of-plane failure: relative tangential stress (left) versus relative shear stress (right).

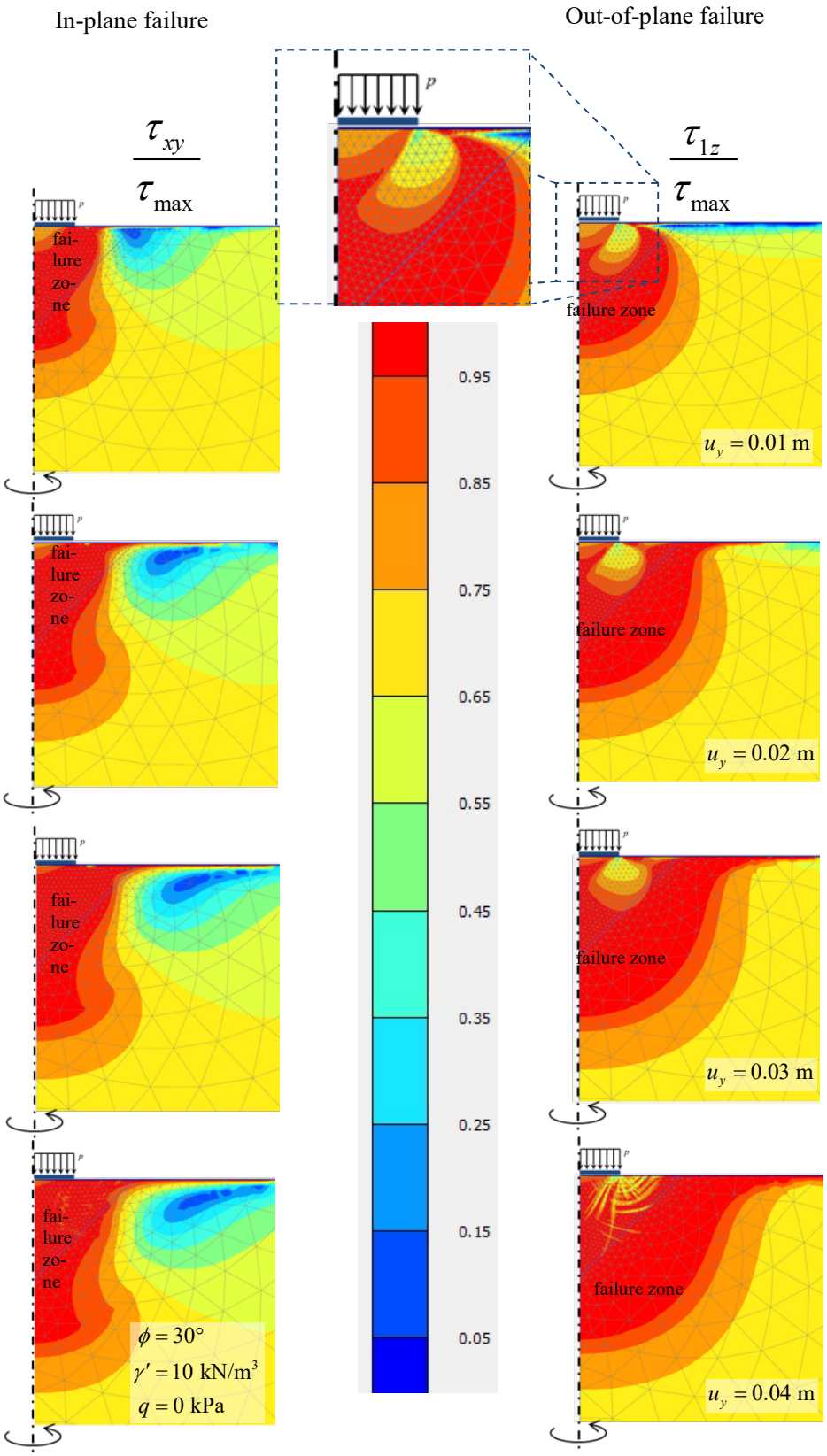


Fig. 8. Soil-weight Case: Relative shear stress (left: in-plane; right: out-of-plane).

Figure 8 shows the results for the soil-weight component, in which a non-cohesive soil has been used with effective self-weight $\gamma'$ = 10 kN/m$^3$, and without a surcharge. The figure shows, for a circular shallow foundation, the relative shear stresses for the "in-plane" direction (on the left) and the "out-of-plane" direction (on the right). Just as for the Surcharge Case (Figure 6) there is both in-plane and out-of-plane failure, but most of the failure is out-of-plane failure (failure zone is much bigger). Also after some deformation the thin shear lines appear. So, just as for the Surcharge Case, this failure mechanism is different from the Prandtl-wedge failure mechanism.

## 4. Failure mechanism of circular pile foundations

### 4.1. *Numerical simulation*

In order to check the axisymmetric failure mechanism for pile foundations, additional finite element calculations have been made with Plaxis 2D. A Mohr-Coulomb soil model has been used for a fine, wide mesh with 15-node elements. The soil has a Young's modulus of $E$ = 50 MPa and a Poisson's ratio of $\nu$ = 0.3. The groundwater level is at the ground surface. The pile has a high Young's modulus of $E$ = 30 GPa, a Poisson's ratio of $\nu$ = 0.10, and roughness coefficient of $R$ = 0.70. The pile has a radius of 0.20 m and is 10 m long.

### 4.2. *Results: in-plane versus out-of-plane failure zones*

The failure mechanism for pile foundations can be studied in the same way as for shallow foundations.

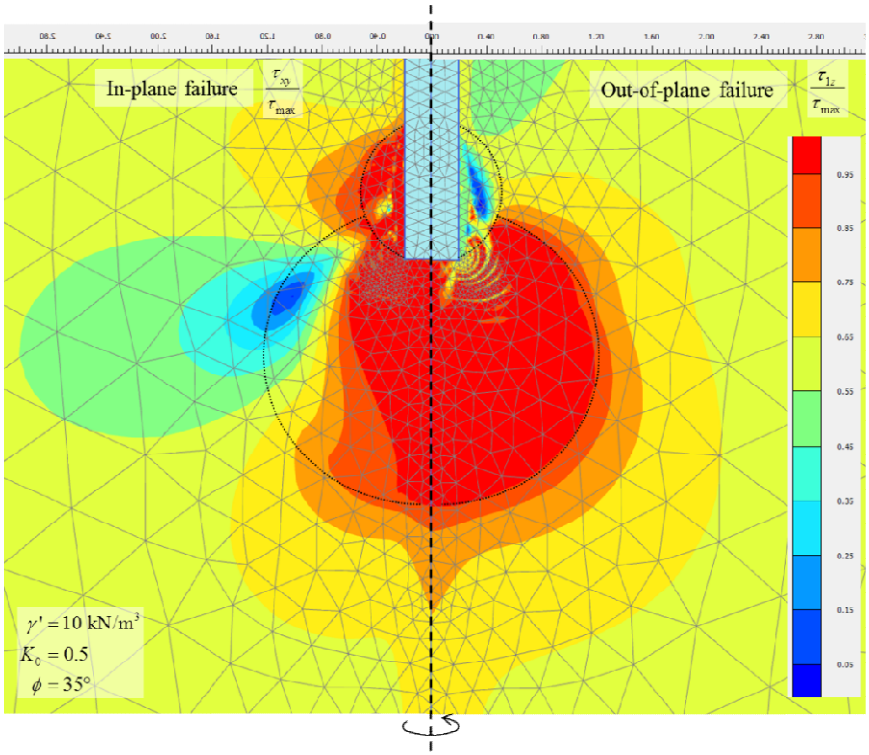


Fig. 9. Relative shear stress, around the pile tip (left: in-plane; right: out-of-plane).

Figure 9 shows, for a circular pile foundation, the relative shear stresses for both the *x-y* plane (in-plane), and also out of this plane (out-of-plane). This figure shows that there is failure both in-pane and out-of-plane, but most of the failure is due to out-of-plane failure (the failure zone is much bigger). The only zone where this is the opposite, is the zone just above the pile tip, around the pile; here there is mostly in-plane failure. The zone with (in- or out-of-plane) failure is round as a ball, just as in Figure 5. So, also for pile foundations, the failure mechanism is different from the Prandtl-wedge failure mechanism, but shows great similarities with the axisymmetric failure mechanism of a shallow foundation.

### 4.3. *Results: tangential stress, shear stress and shear strain*

Also interesting in figure 9 are the circular thin zones around the pile tip, where there is no out-of-plane failure (but still in-plane failure!). The explanation for this follows from figure 10. This figure shows the relative tangential stress versus relative shear stress, around the pile tip. At the thin circular zones without out-of-plane failure, the tangential (out-of-plane) stresses are relatively high.

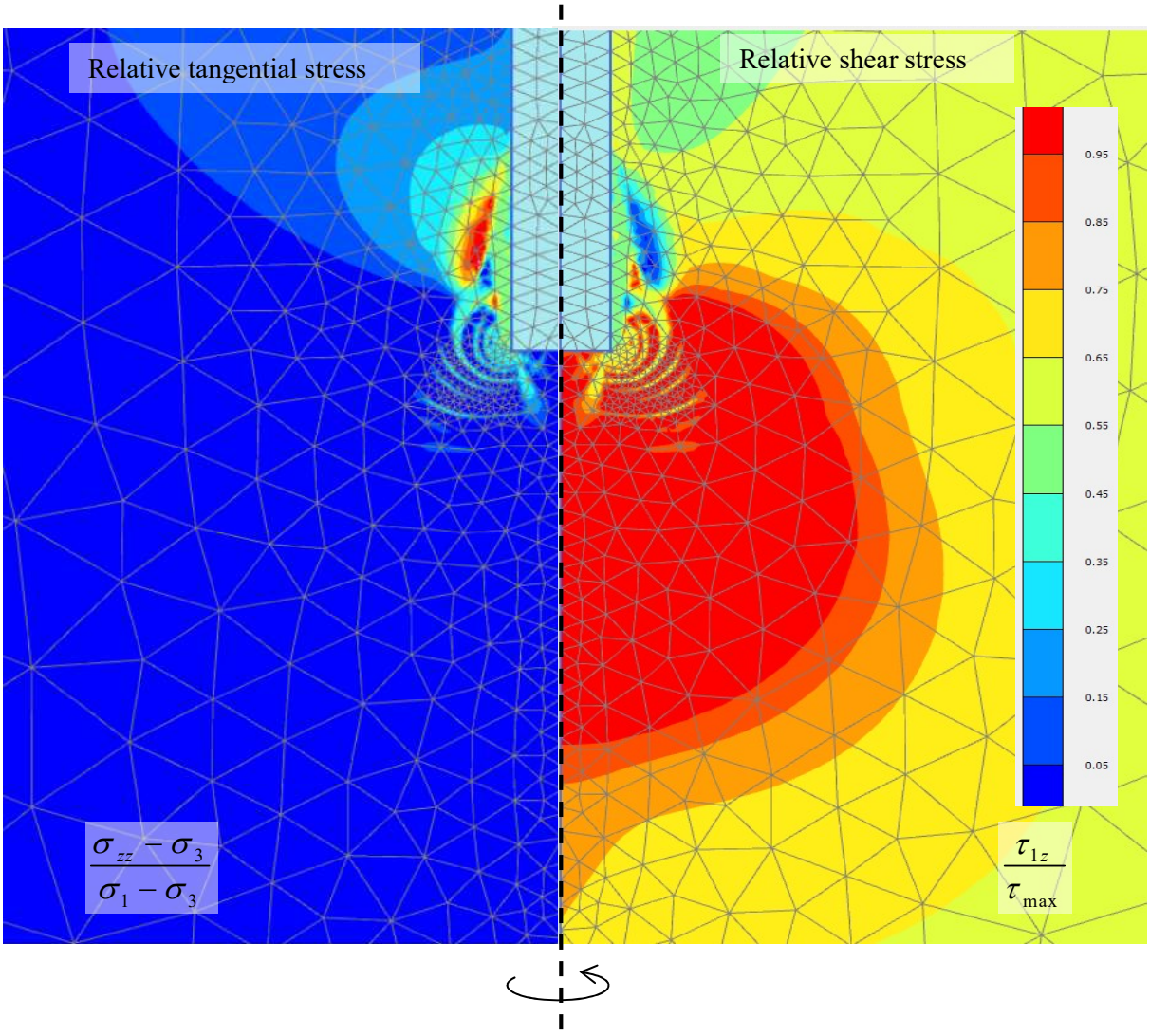


Fig. 10. Relative tangential stress versus relative shear stress, around the pile tip.

Figure 11 shows the reason for the relatively high tangential (out-of-plane) stresses. The zones of the relatively high tangential (out-of-plane) stresses or relatively low shear stresses (figure 11 on the right), are exactly the zones of relatively large (in plane) shear strains (figure 11 on the left). These shear lines can also be found in the figures 6, 7 and 8 for shallow foundations. These shear zones are created, because the inner circles rotate faster than the outside circles of the soil below the pile tip. So it seems that, this in-plane shearing or sliding allows the soil also to shear partially in tangential direction (the lowest stress direction), which increases the stresses in tangential direction.

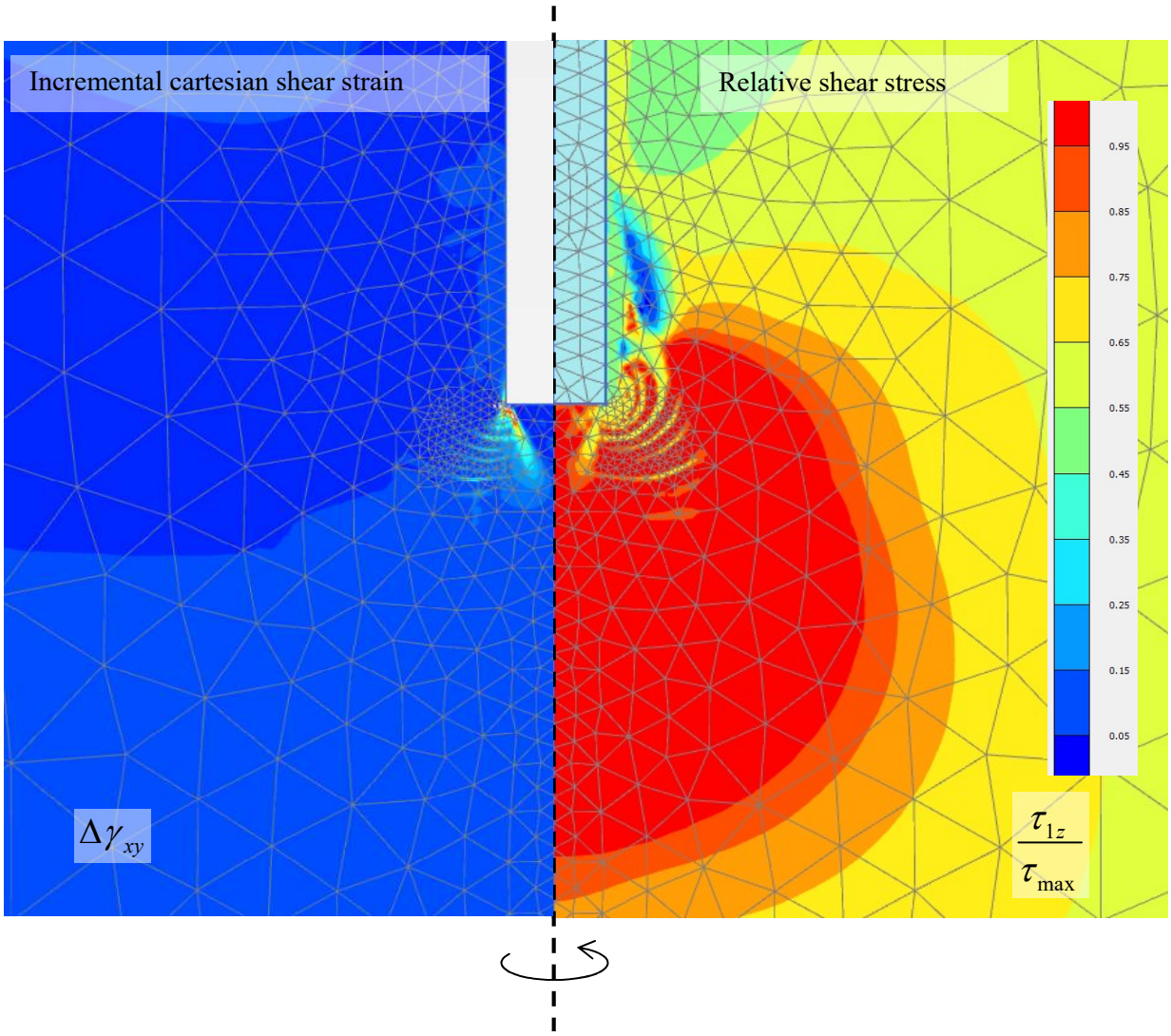


Fig. 11. Incremental shear strain versus relative shear stress, around the pile tip.

## 5. Conclusions

The numerical calculations made in this article show that the failure zone (plastic zone) below a loaded circular plate or pile tip, is far wider and deeper than a Prandtl-wedge. These calculations also show that there is, for these axisymmetric cases, failure both in and out of the standard *x-y* plane, but the out-of-plane (tangential) failure zone is clearly

larger than the in-plane failure zone. Therefore, this failure mechanism is different from the Prandtl-wedge failure mechanism.

Also interesting are the circular and diagonal thin zones below the plate and around the pile tip, where there is no out-of-plane failure (but still in-plane failure!). The reason for the existence of these zones is that, in these thin zones without out-of-plane failure, the tangential (out-of-plane) stresses are relatively high. The relatively high tangential (out-of-plane) stresses in these zones are caused by the relatively large shear strains. In these thin zones, the soil is shearing or sliding, because the inner circles rotate faster than the outside circles of soil below the pile tip. This shearing or sliding allows the soil also to shear partially in tangential direction (because it is the direction with the lowest stress), which increases the stresses in tangential direction.

## Conflict of Interests

The author declares that there is no conflict of interests regarding the publication of this paper.

## References

Brinch Hansen, J. A. (1970). Revised and extended formula for bearing capacity, Bulletin, Danish Geotechnical Institute Copenhagen, 28m 5-11.

Caquot, A., and Kerisel, J. (1953). Sur le terme de surface dans le calcul des fondations en milieu pulverulent. Proc. Third International Conference on Soil Mechanics and Foundation Engineering, Zurich, Switzerland, 1, 336–337.

Caquot, A., and Kerisel, J. (1966) Traité de Méchanique des sols, Gauthier-Villars, Paris, 349, 353, 391.

Chen, W. F. (1975). Limit analysis and soil plasticity, Elsevier, Amsterdam, the Netherlands.

De Beer, E. E. and Ladany, B. (1961) Etude expérimentale de la capacité portante du sable sous des fondations circulaire établies en surface, Proceedings 5th International Conference on Soil Mechanics and Foundation Engineering, Paris, 1, 577-581

De Beer, E. E. (1967) Proefondervindelijke bijdrage tot de studie van het grensdraagvermogen van zand onder funderingen op staal; Bepaling van de vormfactor $s_b$, Annales des Travaux Publics de Belgique, 68, No.6, 481-506; 69, No.1, 41-88; No.4, 321-360; No.5, 395-442; No.6, 495-522. [In Dutch]

De Beer, E. E. (1970) Experimental determination of the shape factors and the bearing capacity factors of sand. Géotechnique, 20, 4, 387-411.

Fang, Hsai-Yang (1990) Foundation Engineering Handbook, Kluwer, Norwell-USA / Dordrecht, the Netherlands.

Jumikis, A. R. (1956). Rupture surfaces in sand under oblique loads, Journal of Soil Mechanics and Foundation Design, ASCE, 82, 1, 1-26

Keverling Buisman, A. S. (1935). De Weerstand van Paalpunten in Zand. De Ingenieur, 50 (Bt. 25–28), 31-35. [In Dutch]

Keverling Buisman, A. S. (1940). Grondmechanica, Waltman, Delft, the Netherlands, 227, 243.

Knudsen, B. S. and Mortensen, N. (2016). Bearing capacity comparison of results from FEM and DS/EN 1997-1 DK NA 2013, Northern Geotechnical Meeting 2016, Reykjavik, 577-586

Loukidis, D., Chakraborty, T., and Salgado, R., (2008). Bearing capacity of strip footings on purely frictional soil under eccentric and inclined loads, Canadian Geotechechnical Journal, 45, 768–787

Meyerhof, G. G. (1951). The ultimate bearing capacity of foundations, Géotechnique, 2, 301-332

Meyerhof, G. G. (1953). The bearing capacity of foundations under eccentric and inclined loads, in Proc. III intl. Conference on Soil Mechanics and Foundation Engineering, Zürich, Switzerland, 1, 440-445

Meyerhof, G. G. (1963). Some recent research on the bearing capacity of foundations, Canadian Geotechnical Journal, 1(1), 16-26

Meyerhof, G. G. (1965). Shallow foundations, Journal of the Soil Mechanics and Foundations Division ASCE, Vol. 91, No. 2, March/April 1965, 21-32

Muhs, H. and Weiß, K. (1972). Versuche über die Standsicheheit flach gegründeter Einzelfundamente in nichtbindigem Boden, Mitteilungen der Deutschen Forschungsgesellschaft für Bodenmechanik (Degebo) an der Technischen Universität Berlin, Heft 28, 122

Prandtl, L. (1920). Über die Härte plastischer Körper. Nachrichten von der Gesellschaft der Wissenschaften zu Göttingen, Mathematisch-Physikalische Klasse, 74–85.

Reissner, H. (1924). Zum Erddruckproblem. Proc., 1st Int. Congress for Applied Mechanics, C. B. Biezeno and J. M. Burgers, eds., Delft (the Netherlands), 295–311.

Selig, E. T. and McKee, K. E. (1961). Static behavior of small footings, Journal of Soil Mechanics and Foundation Design, ASCE, 87, 29-47

Terzaghi, K. (1943). Theoretical soil mechanics, J. Wiley, New York, USA.

Van Baars, S. (2014) The inclination and shape factors for the bearing capacity of footings, Soils and Foundations, 54, 5, 985-992

Van Baars, S. (2015). The Bearing Capacity of Footings on Cohesionless Soils, The Electronic Journal of Geotechnical Engineering, Vol 20, No 26

Van Baars, S. (2016). Failure mechanisms and corresponding shape factors of shallow foundations, Proc. 4th Int. Conf. on New Development in Soil Mech. and Geotechn. Eng., Nicosia, Cypres, 551-558

Van Mierlo, J.C. and Koppejan, A.W. (1952) Lengte en draagvermogen van heipalen, Bouw, No. 3.

Vesic, A. S. (1967) A study of bearing capacity of deep foundations, Final Report Project B-189, Georgia Institute of Technology, Atlanta, 231-236

Vesic, A. S. (1973). Analysis of ultimate loads of shallow foundations. Journal of Soil Mechanics and Foundation Division, 99(1), 45–76.

Vesic, A. S. (1975). Bearing capacity of shallow foundations, H.F. Winterkorn, H.Y. Fang (Eds.), Foundation Engineering Handbook, Van Nostrand Reinhold, New York, USA, 121–147